Estimation of elastic stiffness parameters in weakly anisotropic rotated HTI media

David Cho and Gary F. Margrave

ABSTRACT

The presence of fractures and directional in-situ stress fields in the subsurface has profound implications for numerous geophysical and engineering applications. These phenomenon manifest as azimuthal variations in the seismic response and can be detected in the amplitudes of the scattered wavefield. Therefore, the study of the azimuthal amplitude variation with offset (AVO) can provide information regarding the fracturing or the stress state of the subsurface.

In this study, a transversely isotropic medium with a horizontal axis of symmetry (HTI) was used to model the presence of fractures and directional in-situ stress fields. Previous formulations of the reflections from HTI media invoke conditions that are often unrealistic in the natural world. Therefore, a more generic HTI reflection model was presented. This involves a transformation of the elastic stiffness matrix to represent an unknown symmetry axis azimuth where it is allowed to vary as a function of depth. In addition, we investigate the effect of dipping fracture sets and when the vertical stress is not equal to one of the principle stresses. It is shown that the corresponding reflection coefficients for a transformed HTI medium is capable of resolving the symmetry axis azimuth but lacks the complete set of parameters required to characterize the dipping fractures or when the vertical stress is not equal to one of the principle stresses. However, a different parameterization of the model space in the parameter estimation problem can provide an inference as to the presence of dipping fractures or a non-vertical principle stress component. These concepts are illustrated through a numerical example.

INTRODUCTION

Characterization of azimuthally anisotropic media has been the subject of considerable interest in recent years due to the increased exploration of unconventional resources. Whether the anisotropy is due to fracturing or directional in-situ stress fields, it has profound implications in numerous geophysical and engineering applications. For example, oriented fracture sets can influence the permeability pathways in subsurface formations and the in-situ stress field can influence the fracture response in hydraulic stimulation.

Subject to the assumption that linear elasticity holds, analysis of the stress and strain relationship will yield the elastic stiffness parameters that characterize the medium. In a reflection seismic experiment, stresses imposed on the medium by the incident wavefield result in strains that excite particle motion that can be detected by the scattered wavefield. Therefore, analysis of the reflection coefficient or azimuthal amplitude variation with offset (AVO) provides the means to estimate the medium parameters. These parameters can then be used to infer the presence of fractures (Schoenberg and Sayers, 1995) or determine the in-situ stress field (Gray, 2010).

A transversely isotropic medium with a horizontal axis of symmetry (HTI) provides a simple model for the description of a parallel vertical fracture system or the presence of directional horizontal stresses where the vertical and maximum horizontal stresses are assumed equal. The properties of P wave reflection in HTI media have been discussed in detail in the literature. For example, Haugen and Ursin (1996) derived approximate P wave reflection coefficients for an interface separating a transversely isotropic medium with a vertical axis of symmetry (VTI) from an HTI medium and Rüger (1998) derived approximate formulas for an interface separating two HTI media. However, the models presented are often constrained to measurement profiles in the symmetry planes and invoke conditions that are often unrealistic in the natural world. Therefore, the discussion here is to present a more representative model for P wave reflection in HTI media and discuss the implications for the parameter estimation problem.

HTI MEDIA UNDER A COORDINATE ROTATION

Consider a medium that exhibits HTI symmetry as shown in Figure 1. The HTI model has an axis of rotational symmetry normal to the fracture plane or along the direction of minimum horizontal stress for the fracture and stress models respectively. This is referred to as the symmetry axis. The natural coordinate system of the medium is then one where the symmetry axis is coincident with the x_1 axis.

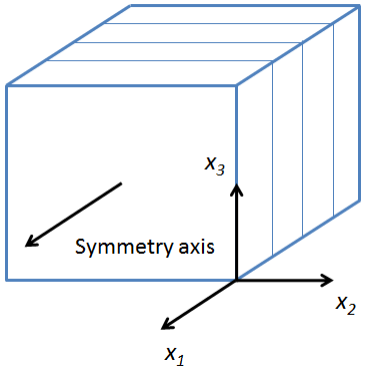

FIG. 1. HTI media in its natural coordinate system where the symmetry axis coincides with the x_1 axis.

Here we use the Voigt notation $A_{\alpha\beta}$ rather than the tensor notation a_{ijkl} for the density normalized elastic stiffness parameters, with α and β running from 1 to 6 and i, j, k and l running from 1 to 3. From here on in, the density normalized elastic stiffness parameters will be referred to as the elastic stiffness parameters. The elastic stiffness matrix for the configuration in Figure 1 is given by

$$\underline{\underline{A^n}} = \begin{bmatrix} A_{11}^n & A_{12}^n & A_{13}^n & 0 & 0 & 0 \\ A_{12}^n & A_{22}^n & A_{23}^n & 0 & 0 & 0 \\ A_{13}^n & A_{23}^n & A_{33}^n & 0 & 0 & 0 \\ 0 & 0 & 0 & A_{44}^n & 0 & 0 \\ 0 & 0 & 0 & 0 & A_{55}^n & 0 \\ 0 & 0 & 0 & 0 & 0 & A_{66}^n \end{bmatrix}, \tag{1}$$

where the following symmetry relations are satisfied:

$$A_{33}^n = A_{22}^n, \;\; A_{55}^n = A_{66}^n, \;\; A_{13}^n = A_{12}^n, \;\; A_{23}^n = A_{33}^n - 2A_{44}^n . \tag{2}$$

The superscript *n* denotes the elastic stiffness parameters are in its natural coordinate system. Since the elastic stiffness matrix is symmetric, equation 1 consists of nine non-vanishing components of the elastic stiffness parameters where five are independent as governed by the relations in equation 2. We note that the conditions in equations 1 and 2 are only applicable if the reference coordinate system coincides with the natural coordinate system.

Let us now investigate the effect of a reference coordinate system that does not coincide with the natural coordinate system. We demonstrate this by investigating the effect of an elastic stiffness matrix that undergoes a coordinate transformation. In the interest of economy of space and efforts in algebraic manipulation, the coordinate transformation is performed by employing a matrix technique purposed by Bond (1943) to avoid converting to full subscripts. It involves the construction of a matrix operator to be used in transforming stress and strain by a single matrix multiplication. The corresponding result for the rotation of the elastic stiffness matrix is

$$\underline{\underline{A}} = \underline{\underline{M}}\,\underline{\underline{A^n}}\,\underline{\underline{M^T}}, \tag{3}$$

where A represents the rotated elastic stiffness matrix and M represents the Bond transformation matrix and is a function of an operator containing the directional cosines for the desired rotation (see Bond, 1943). In the following, we investigate the effect of a coordinate rotation about the x_2 and the x_3 axes.

Coordinate rotation about the x_2 axis

Consider a rotation of the coordinate system about the x_2 axis by an angle ξ as in Figure 2. This scenario represents the condition for dipping fracture planes or when the vertical stress is not equal to one of the principle stresses. This condition represents areas of structure and in the vicinity of faults.

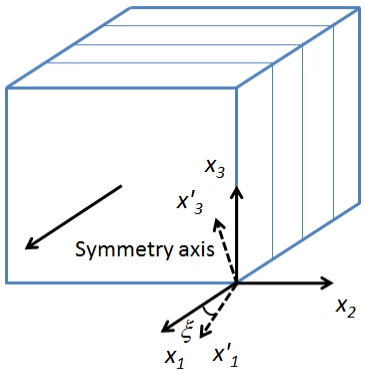

FIG. 2. HTI media under a coordinate rotation about the x_2 axis by an angle ξ.

The Bond (1943) transformation matrix for a rotation about the x_2 axis by an angle ξ is given by

$$\underline{\underline{M(\xi)}} = \begin{bmatrix} \cos^2\xi & 0 & \sin^2\xi & 0 & -\sin 2\xi & 0 \\ 0 & 1 & 0 & 0 & 0 & 0 \\ \sin^2\xi & 0 & \cos^2\xi & 0 & \sin 2\xi & 0 \\ 0 & 0 & 0 & \cos\xi & 0 & \sin\xi \\ \frac{\sin 2\xi}{2} & 0 & -\frac{\sin 2\xi}{2} & 0 & \cos 2\xi & 0 \\ 0 & 0 & 0 & -\sin\xi & 0 & \cos\xi \end{bmatrix}, \tag{4}$$

and the resulting elastic stiffness matrix in the rotated coordinate system takes the form

$$\underline{\underline{A(\xi)}} = \begin{bmatrix} A_{11}(\xi) & A_{12}(\xi) & A_{13}(\xi) & 0 & A_{15}(\xi) & 0 \\ A_{12}(\xi) & A_{22}(\xi) & A_{23}(\xi) & 0 & A_{25}(\xi) & 0 \\ A_{13}(\xi) & A_{23}(\xi) & A_{33}(\xi) & 0 & A_{35}(\xi) & 0 \\ 0 & 0 & 0 & A_{44}(\xi) & 0 & A_{46}(\xi) \\ A_{15}(\xi) & A_{25}(\xi) & A_{35}(\xi) & 0 & A_{55}(\xi) & 0 \\ 0 & 0 & 0 & A_{46}(\xi) & 0 & A_{66}(\xi) \end{bmatrix}. \tag{5}$$

Note the appearance of A_{15}, A_{25}, A_{35} and A_{46}. The non-vanishing components of the elastic stiffness matrix now consist of 13 parameters.

Coordinate rotation about the x_3 axis

Next consider a rotation of the coordinate system about the x_3 axis by an angle ψ as in Figure 3. This scenario represents the typical case for fracture detection or stress estimation where the symmetry axis azimuth is unknown.

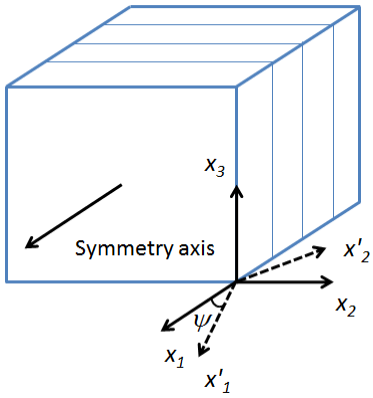

FIG. 3. HTI media under a coordinate rotation about the x_3 axis by an angle ψ.

The Bond (1943) transformation matrix for a rotation about the x_3 axis by an angle ψ is given by

$$\underline{\underline{M(\psi)}} = \begin{bmatrix} \cos^2\psi & \sin^2\psi & 0 & 0 & 0 & \sin 2\psi \\ \sin^2\psi & \cos^2\psi & 0 & 0 & 0 & -\sin 2\psi \\ 0 & 0 & 1 & 0 & 0 & 0 \\ 0 & 0 & 0 & \cos\psi & -\sin\psi & 0 \\ 0 & 0 & 0 & \sin\psi & \cos\psi & 0 \\ -\dfrac{\sin 2\psi}{2} & \dfrac{\sin 2\psi}{2} & 0 & 0 & 0 & \cos 2\psi \end{bmatrix}, \tag{6}$$

and the resulting elastic stiffness matrix in the rotated coordinate system takes the form

$$\underline{\underline{A(\psi)}} = \begin{bmatrix} A_{11}(\psi) & A_{12}(\psi) & A_{13}(\psi) & 0 & 0 & A_{16}(\psi) \\ A_{12}(\psi) & A_{22}(\psi) & A_{23}(\psi) & 0 & 0 & A_{26}(\psi) \\ A_{13}(\psi) & A_{23}(\psi) & A_{33}(\psi) & 0 & 0 & A_{36}(\psi) \\ 0 & 0 & 0 & A_{44}(\psi) & A_{45}(\psi) & 0 \\ 0 & 0 & 0 & A_{45}(\psi) & A_{55}(\psi) & 0 \\ A_{16}(\psi) & A_{26}(\psi) & A_{36}(\psi) & 0 & 0 & A_{66}(\psi) \end{bmatrix}. \tag{7}$$

Note the appearance of A_{16}, A_{26}, A_{36} and A_{45}. As in the case of a rotation about the x_2 axis, the non-vanishing components of the elastic stiffness matrix now consist of 13 parameters.

The individual equations representing each elastic stiffness parameter in the rotated coordinate system are not shown here due to spatial constraints. They consist of various combinations of sinusoidal functions and the elastic stiffness parameters in the natural coordinate system. Therefore, no simple symmetries can be invoked once the reference coordinate system deviates from the natural coordinate system. The application of a rotational operator results in a distribution of elastic stiffness parameters to specific locations in the matrix depending on the nature of the rotation. Note that in the above

representation of the rotated elastic stiffness matrix for HTI media (equations 5 and 7), the symmetry relations in its natural coordinate system as given by equation 2 were not invoked. Therefore, the discussion thus far can be generalized to an orthorhombic medium with nine independent non-vanishing elastic stiffness parameters in its natural coordinate system.

RELECTION COEFFICIENTS FOR WEAKLY ANISOTROPIC HTI MEDIA

Approximate scattering coefficients have been derived by various authors using perturbation techniques (i.e. Thomsen, 1993, Rüger, 1998 and Vavryčuk and Pšenčík, 1998). The basis for perturbation theory is to obtain an approximate solution for a problem which cannot be solved exactly. This is achieved by the addition of "small" perturbation terms to the description of a similar exactly solvable problem. In the case of approximate reflection coefficients in anisotropic media, the perturbations represent the anisotropic deviation from a solvable isotropic background. The "small" perturbations therefore dictate a weak contrast interface separating two weakly anisotropic media. However, according to Thomsen (1993), this condition is valid for most reflecting interfaces and therefore the assumption of a weak contrast interface is appropriate.

In the following, we investigate two scenarios for the reflection of P waves from an interface separating two homogeneous HTI half-spaces. The first is a model discussed in Rüger (1998) where the upper and lower HTI half-spaces have the same symmetry axis azimuth above and below the interface. The second is a more generic scenario where the upper and lower HTI half-spaces each have an arbitrary symmetry axis azimuth. Figure 4 shows the two scenarios.

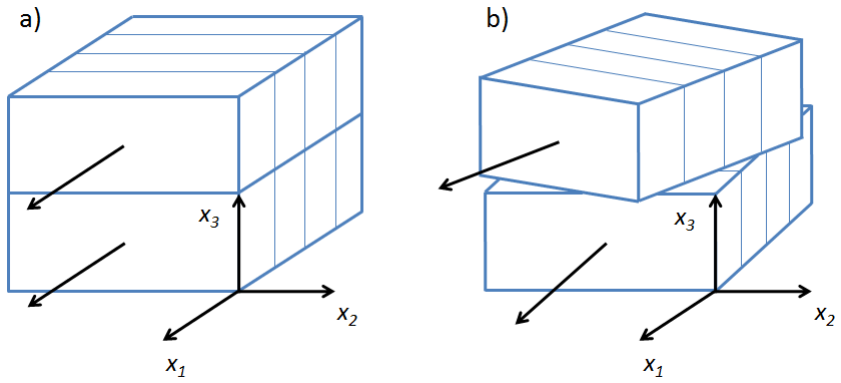

FIG. 4. HTI/HTI interface with a) similar symmetry axis orientations and b) arbitrary symmetry axis orientations.

HTI/HTI interface with similar symmetry axis orientations

For the case of the HTI/HTI interface with the same symmetry axis azimuth above and below the interface (Figure 4a), the P wave reflection coefficient in the natural coordinate system of the medium is given by (Rüger, 1998)

$$R_{pp}(\theta,\phi) = \frac{1}{2}\frac{\Delta Z}{\overline{Z}} + \frac{1}{2}\left[\frac{\Delta\alpha}{\overline{\alpha}} - \left(\frac{2\overline{\beta}}{\overline{\alpha}}\right)^2 \frac{\Delta G}{\overline{G}}\right.$$
$$+ \left[\Delta\left(\frac{(A_{13}^n + A_{55}^n)^2 - (A_{33}^n + A_{55}^n)^2}{2A_{33}^n(A_{33}^n + A_{55}^n)}\right) + 2\left(\frac{2\overline{\beta}}{\overline{\alpha}}\right)^2 \Delta\left(\frac{(A_{44}^n - A_{66}^n)}{2A_{66}^n}\right)\right]\cos^2\phi\left.\right]\sin^2\theta$$
$$+ \frac{1}{2}\left[\frac{\Delta\alpha}{\overline{\alpha}} + \Delta\left(\frac{(A_{11}^n - A_{33}^n)}{2A_{33}^n}\right)\cos^4\phi\right.$$
$$\left. + \Delta\left(\frac{(A_{13}^n + A_{55}^n)^2 - (A_{33}^n + A_{55}^n)^2}{2A_{33}^n(A_{33}^n + A_{55}^n)}\right)\sin^2\phi\cos^2\phi\right]\sin^2\theta\tan^2\theta \quad , \qquad (8)$$

where α and β are the P and S wave velocities respectively, $Z=\rho\alpha$ is the acoustic impedance, $G=\rho\beta^2$ is the shear modulus, ρ is the density, θ is the angle of incidence and ϕ is the measurement azimuth. The bar represents an averaging of the values (i.e. $\overline{w} = \frac{1}{2}[w_2+w_1]$) and Δ represents a difference of the values (i.e. $\Delta w = w_2-w_1$) above and below the reflecting interface. Equation 6 corresponds exactly to equation 5 of Rüger (1998) with the exception that the elastic stiffness parameters were used instead of anisotropy parameters.

If the symmetry axis azimuth is unknown, the measurement azimuth ϕ is expressed as the difference between the azimuthal direction of the k^{th} observed azimuth and the direction of the symmetry axis ϕ_{sym} (Rüger, 1998). The AVO gradient (i.e. angle dependent) term in equation 6 is then defined as

$$B(\phi_k) = B^{iso} + B^{ani}\cos^2(\phi_k - \phi_{sym}), \qquad (9)$$

with

$$B^{iso} = \frac{1}{2}\left[\frac{\Delta\alpha}{\overline{\alpha}} - \left(\frac{2\overline{\beta}}{\overline{\alpha}}\right)^2 \frac{\Delta G}{\overline{G}}\right] \qquad (10)$$

and

$$B^{ani} = \frac{1}{2}\left[\Delta\left(\frac{(A_{13} + A_{55})^2 - (A_{33} + A_{55})^2}{2A_{33}(A_{33} + A_{55})}\right) + 2\left(\frac{2\overline{\beta}}{\overline{\alpha}}\right)^2 \Delta\left(\frac{(A_{44}^n - A_{66}^n)}{2A_{66}^n}\right)\right]. \qquad (11)$$

Equation 9 can be used to determine the symmetry axis azimuth by solving for ϕ_{sym}. However, due to the nonlinearity of equation 9, the solution for ϕ_{sym} is non-unique and will yield two possible directions for the symmetry axis orthogonal to one another (Rüger, 1998). In addition, since the symmetry axis above and below the interface must have a similar azimuth, for a multi-layered Earth, this model implies that the symmetry axis azimuth is invariant with depth. To overcome this issue, numerous authors have imposed the condition of an isotropic overburden. The above scenarios however, pose an

unrealistic constraint and therefore, a more generic HTI reflection model is required for a more accurate description.

HTI/HTI interface with arbitrary symmetry axis orientations

To remove the constraint of an invariant symmetry axis azimuth with depth, an HTI/HTI interface with an arbitrary symmetry axis azimuth above and below the interface is considered (Figure 4b). As discussed above, HTI media rotated about the x_3 axis must be regarded as an anisotropic medium with non-vanishing elastic stiffness parameters given by equation 5.

Vavryčuk and Pšenčík (1998) derived P wave reflection coefficients for weak contrast interfaces separating two weakly but arbitrarily anisotropic media. As a result of the perturbation theory, the formula depends on the choice of parameters (P and S wave velocities) used for the background isotropic medium. A discussion of the effects for various background velocities can be found in Pšenčík and Martins (2001). Here, the background P and S wave velocities were chosen to be $\alpha^2=A_{33}$ and $\beta^2=A_{44}$ respectively. These are the vertical P wave velocity and the vertical S wave velocity with a polarization orthogonal to the symmetry axis. The P wave reflection coefficient is then given by

$$
\begin{aligned}
R_{PP}(\theta,\phi) = R_{PP}^{iso}(\theta) + \frac{1}{2}\Bigg[& \Delta\left(\frac{A_{23}+2A_{44}-A_{33}}{A_{33}}\right)\sin^2\phi \\
& + \left(\Delta\left(\frac{A_{13}+2A_{55}-A_{33}}{A_{33}}\right) - 8\Delta\left(\frac{A_{55}-A_{44}}{2A_{33}}\right)\right)\cos^2\phi \\
& + 2\left[\Delta\left(\frac{A_{36}-A_{45}}{A_{33}}\right) - 4\Delta\left(\frac{A_{45}}{A_{33}}\right)\right]\cos\phi\sin\phi\Bigg]\sin^2\theta \\
& + \frac{1}{2}\Bigg[\Delta\left(\frac{A_{11}-A_{33}}{2A_{33}}\right)\cos^4\phi + \Delta\left(\frac{A_{22}-A_{33}}{2A_{33}}\right)\sin^4\phi \\
& + \Delta\left(\frac{A_{12}+2A_{66}-A_{33}}{A_{33}}\right)\cos^2\phi\sin^2\phi + 2\Delta\left(\frac{A_{16}}{A_{33}}\right)\cos^3\phi\sin\phi \\
& + 2\Delta\left(\frac{A_{26}}{A_{33}}\right)\sin^3\phi\cos\phi\Bigg]\sin^2\theta\tan^2\theta
\end{aligned}
, \qquad (12)
$$

where

$$
R_{PP}^{iso}(\theta) = \frac{1}{2}\frac{\Delta Z}{\overline{Z}} + \frac{1}{2}\left[\frac{\Delta\alpha}{\overline{\alpha}} - \left(\frac{2\overline{\beta}}{\overline{\alpha}}\right)^2\frac{\Delta G}{\overline{G}}\right]\sin^2\theta + \frac{1}{2}\frac{\Delta\alpha}{\overline{\alpha}}\sin^2\theta\tan^2\theta . \qquad (13)
$$

Equation 12 consists of an isotropic term with the addition of a perturbation term to account for anisotropy. The isotropic term given by equation 13 is the well-known Aki and Richards (1980) approximate AVO equation for P wave reflection. The anisotropic

correction term consists of various combinations of 13 elastic stiffness parameters called weak anisotropy parameters. These are manifestations of the natural coupling of elastic stiffness parameters that govern wave propagation. Note that the reflection coefficient does not depend on elastic parameters A_{14}, A_{15}, A_{24}, A_{25}, A_{34}, A_{35}, A_{46} and A_{56}. Therefore, these parameters can never be recovered from a P wave reflection experiment (Vavryčuk and Pšenčík, 1998).

THE PARAMETER ESTIMATION PROBLEM

Downton and Roure (2010) described an approach for the estimation of fracture parameters using a simulated annealing technique similar to that of Coulon et al. (2006). Through forward modeling, the simulated annealing algorithm perturbs an initial model until a minimized misfit is achieved between the synthetic and real data. In their formulation of the parameter estimation problem, an HTI model was implemented where the anisotropy is assumed to be the result of a vertical fracture system with an unknown symmetry axis azimuth. The parameterization of the model space is then in terms of the layer time thickness, P and S wave impedances, density, the Thomsen parameters delta, epsilon and gamma and the azimuth of the symmetry axis. They further demonstrated that the number of free parameters that must be estimated could be reduced through the implementation of a rock physics model. For example, the linear slip deformation model (LSD) of Schoenberg and Sayers (1995) or the penny-shaped crack model of Hudson et al. (1981) can be applied. The elastic stiffness matrix is subsequently constructed and the Bond transformation (rotation about the x_3 axis) is applied to allow for the symmetry axis azimuth to vary. Reflection coefficients as a function of incidence angle and azimuth are then calculated and convolved with a source wavelet to generate the synthetic seismograms. Through this approach, the elastic stiffness parameters are estimated through the iterative optimization scheme of the simulated annealing technique.

Equation 12 can be used to implement the forward modeling of the reflection coefficients subject to the assumption that a weak contrast interface separating two weakly anisotropic media holds. Note that in equation 12, the 13 elastic stiffness parameters that describe the reflection coefficient happen to be the same non-vanishing components that describe a rotated HTI or orthorhombic medium about the x_3 axis. However, equation 12 does not include certain elastic stiffness parameters that appear as a result of a rotation about the x_2 axis. This implies that information is present in the P wave reflections for a rotation of an HTI or orthorhombic medium about the x_3 axis but not for the x_2 axis. Therefore, a medium with dipping fractures can never be fully characterized by a P wave reflection experiment.

In addition, all the elastic stiffness parameters in equation 12 can be uniquely defined with the exception of A_{12} and A_{66} where they are coupled through the term $A_{12}+2A_{66}$. In HTI media, A_{12} and A_{66} are non-independent and are equal to A_{13} and A_{55} respectively. Therefore, for the parameter estimation problem, the non-uniqueness of A_{12} and A_{66} do not affect the characterization of HTI media. However, for orthorhombic media, A_{12} and A_{66} are independent and the parameter estimation could result in a false distribution between A_{12} and A_{66}. In this case, an independent measurement is required to validate the solution. For example, A_{66} could be obtained through the analysis of the Stoneley wave mode in borehole sonic measurements (Sinha et al., 2003).

NUMERICAL EXAMPLE

To illustrate the concepts presented above, we consider an HTI medium that undergoes a rotation about the x_2 axis to represent dipping fractures followed by a rotation about the x_3 axis to represent an unknown symmetry axis azimuth. The orientation of the symmetry axis then consists of all three components of the basis vectors that define a Euclidean space. We use case C of the HTI model presented by Vavryčuk and Pšenčík (1998) where the anisotropy of the medium is assumed to be caused by a system of vertical parallel dry cracks. The P and S wave velocities of host rock are 4.0 km/s and 2.3 km/s respectively, the density is 2.6 g/cm^3, the aspect ratio is 10^{-4} and the crack density is 0.05. The corresponding elastic stiffness matrix in its natural coordinate system takes the form

$$\underline{\underline{A^n}} = \begin{bmatrix} 11.96 & 3.99 & 3.99 & 0 & 0 & 0 \\ 3.99 & 15.55 & 4.89 & 0 & 0 & 0 \\ 3.99 & 4.89 & 15.55 & 0 & 0 & 0 \\ 0 & 0 & 0 & 5.33 & 0 & 0 \\ 0 & 0 & 0 & 0 & 4.76 & 0 \\ 0 & 0 & 0 & 0 & 0 & 4.76 \end{bmatrix}, \tag{14}$$

where the units are in (km/s)^2. Now consider a rotation of equation 14 about the x_2 axis by an angle ξ=10 degrees followed by a rotation about the x_3 axis by an angle ψ=30 degrees. The corresponding elastic stiffness matrices are given by

$$\underline{\underline{A(\xi)}} = \begin{bmatrix} 12.05 & 4.02 & 4.00 & 0 & -0.27 & 0 \\ 4.02 & 15.55 & 4.86 & 0 & -0.15 & 0 \\ 4.00 & 4.86 & 15.43 & 0 & -0.35 & 0 \\ 0 & 0 & 0 & 5.31 & 0 & -0.10 \\ -0.27 & -0.15 & -0.35 & 0 & 4.77 & 0 \\ 0 & 0 & 0 & -0.10 & 0 & 4.78 \end{bmatrix} \tag{15}$$

and

$$\underline{\underline{A(\xi,\psi)}} = \begin{bmatrix} 12.84 & 4.10 & 4.22 & 0.05 & -0.25 & 0.71 \\ 4.10 & 14.59 & 4.65 & 0.16 & -0.12 & 0.81 \\ 4.22 & 4.65 & 15.43 & 0.17 & -0.30 & 0.37 \\ 0.05 & 0.16 & 0.17 & 5.18 & 0.23 & -0.07 \\ -0.25 & -0.12 & -0.30 & 0.23 & 4.91 & 0.02 \\ 0.71 & 0.81 & 0.37 & -0.07 & 0.02 & 4.86 \end{bmatrix}. \tag{16}$$

For a rotation about the x_2 followed by the x_3 axes, the elastic stiffness matrix becomes fully populated. However, in a P wave reflection experiment the only parameters that can be recovered are A_{11}, A_{12}, A_{13}, A_{16}, A_{22}, A_{23}, A_{26}, A_{33}, A_{36}, A_{44}, A_{45}, A_{55} and A_{66}. Therefore, the presence of dipping fractures results in information that is forever lost to the non-

retrievable elastic stiffness parameters. What we are left with is a truncated form of equation 16 given by

$$\underline{\underline{A^T(\xi,\psi)}} = \begin{bmatrix} 12.84 & 4.10 & 4.22 & 0 & 0 & 0.71 \\ 4.10 & 14.59 & 4.65 & 0 & 0 & 0.81 \\ 4.22 & 4.65 & 15.43 & 0 & 0 & 0.37 \\ 0 & 0 & 0 & 5.18 & 0.23 & 0 \\ 0 & 0 & 0 & 0.23 & 4.91 & 0 \\ 0.71 & 0.81 & 0.37 & 0 & 0 & 4.86 \end{bmatrix}, \tag{17}$$

where A^T denotes the truncated elastic stiffness matrix.

Now, to recover the orientation of the symmetry axis in the x_1-x_2 plane, we make use of the fact that the difference between the fast and slow polarizations of the vertical S wave velocity must be maximized in its natural coordinate system. Therefore, the symmetry axis orientation in the x_1-x_2 plane can be recovered by searching for the angle ψ such that the condition

$$\max[A^n_{44} - A^n_{55}] \tag{18}$$

is satisfied. Since A^n_{44} and A^n_{55} in a rotation about the x_3 axis are only dependent on A_{44}, A_{45} and A_{55}, equation 17 is sufficient for the recovery to the symmetry axis orientation in the x_1-x_2 plane. Figure 5 shows A_{44}-A_{55} from zero to 180 degrees. The function reaches a maximum at 30 degrees, therefore correctly identifying the orientation of the symmetry axis in the x_1-x_2 plane.

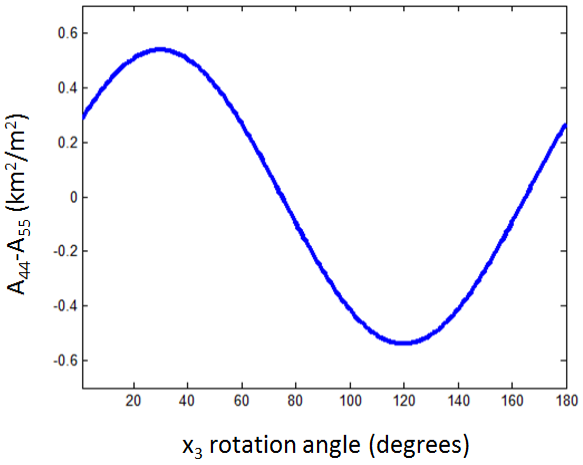

FIG. 5. Plot of A_{44}-A_{55} from zero to 180 degrees. The function reaches a maximum at 30 degrees, denoting the symmetry axis orientation.

The rotation angle in the x_1-x_2 plane can be applied to equation 7 and the corresponding elastic stiffness matrix takes the form

$$\underline{\underline{A^{ne}}} = \begin{bmatrix} 12.05 & 4.02 & 4.00 & 0 & 0 & 0 \\ 4.02 & 15.55 & 4.86 & 0 & 0 & 0 \\ 4.00 & 4.86 & 15.43 & 0 & 0 & 0 \\ 0 & 0 & 0 & 5.31 & 0 & 0 \\ 0 & 0 & 0 & 0 & 4.77 & 0 \\ 0 & 0 & 0 & 0 & 0 & 4.78 \end{bmatrix}, \quad (18)$$

where A^{ne} denotes the equivalent medium as seen by the P waves. Note the form of equation 18 resembles that of an orthorhombic medium. As noted above, a rotation about the x_2 axis results in the appearance of A_{15}, A_{25}, A_{35} and A_{46}. Without knowledge of these elastic stiffness parameters, the elastic stiffness matrix cannot be fully recovered in its natural coordinate system. Therefore, the presence of dipping fractures will result in errors associated with the estimation of elastic stiffness parameters. Figure 6 shows the cumulative errors for all the elastic stiffness parameters as a function of the x_2 rotation angle.

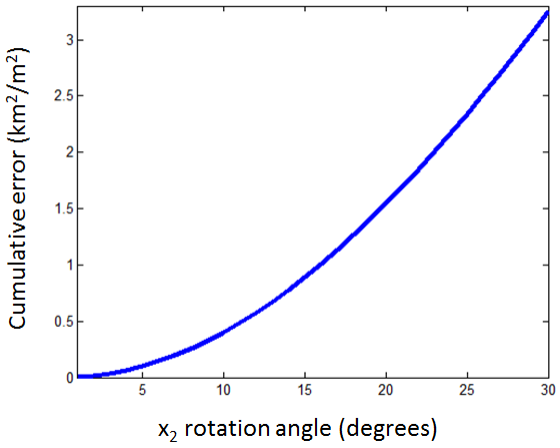

FIG. 6. Cumulative errors for the elastic stiffness parameters as a function of the x_2 rotation angle.

However, if we assume an HTI medium and invoke the conditions as given by equation 2, we can make an inference as to the presence of dipping fractures. Note that the 2,2 component of A^n and A^{ne} are equal. This is due to the fact that this component is invariant under a coordinate rotation about the x_2 axis. A further rotation of this component about the x_3 axis results in a distribution of parameters to recoverable components of the elastic stiffness matrix. Given that A^n_{33} is equal to A^n_{22} for an HTI medium, the deviation of A^{ne}_{33} from A^{ne}_{22} could be used as an indicator for the amount of dip corresponding to the fractures. Therefore, in the parameterization of the model space, an independent estimate of A^{ne}_{33} and A^{ne}_{22} could provide additional information about the medium. Figure 7 shows A^{ne}_{33} - A^{ne}_{22} as a function of the x_2 rotation angle.

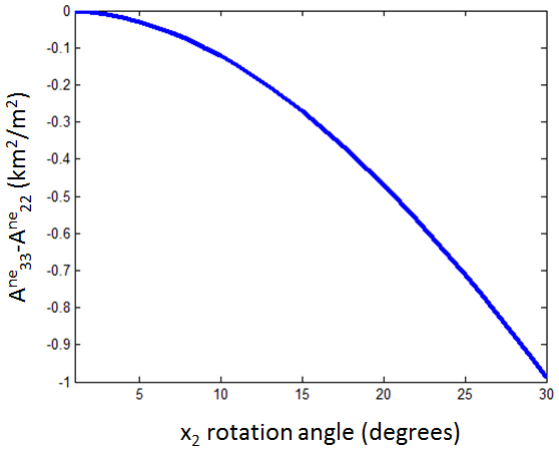

FIG. 7. Plot of A_{33}^{ne} - A_{22}^{ne} as a function of the x_2 rotation angle.

DISCUSSION AND CONCLUSIONS

The estimation of elastic stiffness parameters in weakly anisotropic rotated HTI media was discussed. The bond transformation allows for the representation of HTI media in a reference coordinate system that deviates from its natural coordinate system. This in conjunction with Vavryčuk and Pšenčík's (1998) formulation of the P wave reflection coefficient provides an approach to address the shortcomings of Rüger's (1998) HTI reflection model. Analysis of the rotation of the elastic stiffness matrix and reflection coefficient suggests that the symmetry axis orientation in the x_1-x_2 plane is recoverable from a P wave reflection experiment. Characterization of a medium with dipping fractures or when the vertical stress is not equal to one of the principle stresses is incomplete due to the appearance of elastic stiffness parameters that is not a function of the P wave reflection coefficient. However, if an HTI model is assumed in conjunction with a re-parameterization of the model space, the presence of dipping fractures or the orientation of the principle stresses can be inferred. In addition, if an orthorhombic model is used instead of an HTI model, the non-unique definition of A_{12} and A_{66} requires additional information to validate the solution.

The methodology discussed provides the means to simultaneously estimate both isotropic and anisotropic properties. The isotropic properties provide information concerning reservoir lithologies and fluids whereas the anisotropic properties provide information concerning the fracturing or the differential stress state of the reservoir. As suggested by Norton el al. (2010), the isotropic Poisson's ratio (PR) exhibits a large correlation to the extent of fracture propagation in the hydraulic stimulation of an unconventional shale reservoir, where fracture growth is preferential towards the lower PR regions. The PR can be inversely correlated to the quartz-clay ratio and therefore is an indicator for the material properties of the medium. In addition, a lower PR corresponds to lower horizontal stresses resulting from a vertical lithostatic load, resulting in the preferred fracture growth towards areas of lower PR (Maxwell et al., 2011). The anisotropic properties could then supplement the results by providing information regarding pre-existing fractures or the preferred fracture geometry. In areas where azimuthal anisotropy exists, this could indicate either the presence of existing fractures or

differential horizontal stresses. The differentiation of the two cases would be due to whether failure has occurred or not and could be determined using the Mohr-Coulomb failure criterion. For hydraulic stimulation in areas of pre-existing faults and fractures, fault activation mechanisms could prevail and act as a barrier for fracture propagation (Maxwell et al., 2011). If failure has not occurred, the degree of anisotropy could indicate whether a planar or complex fracture system will initiate. Therefore, knowledge of the isotropic and anisotropic properties is critical in optimizing the development of unconventional resources.

FUTURE WORK

Through the use of numerical and scaled physical models, the concepts discussed above can be further validated. In addition, the concept of stress and strain in elasticity provides a common framework for multi-disciplinary studies. The goal is to integrate various disciplines including seismology, microseismology and geomechanics to achieve an improved characterization of the subsurface.

REFERENCES

Aki, K., Richards, P. G., 1980, Quantitative seismology: W.H. Freeman & Co.

Bond, W., 1943, The mathematics of the physical properties of crystals: BSTJ, 22, 1-72.

Coulon, J.-P., Y. Lafet, B. Deschizeaux, P. M. Doyen, and P. Duboz, 2006, Stratigraphic elastic inversion for seismic lithology discrimination in a turbiditic reservoir: 76th Annual International Meeting, SEG, Expanded Abstracts, 25, no. 1, 2092-2096.

Downton, J., Roure, B., 2010, Azimuthal simultaneous elastic inversion for fracture detection: 80th Annual International Meeting, SEG, Expanded Abstracts, 263-267.

Gray, D., P. Anderson, J. Logel, F. Delbecq, and D. Schmidt, 2010, Principle stress estimation in shale plays using 3D seismic: GeoCanada2010.

Haugen, G. U., and Ursin, B., 1996, AVO-A analysis of vertically fractured reservoir underlaying shale: Presented at the 66th Annual International Meeting, SEG, Expanded Abstracts, 1826–1829.

Hudson, J. A., 1981, Wave speeds and attenuation of elastic waves in material containing cracks: Geophysical Journal of the Royal Astronomical Society, 64, 133–150.

Maxwell, S. C., Cho, D., Pope, T., Jones, M., Cipolla, C., Mack, M., Henery, F., Norton, M., 2011, Enhanced reservoir characterization using hydraulic fracture microseismicity: SPE Hydraulic Fracturing Technology Conference and Exhibition, The Woodlands, Texas, SPE 140449

Norton, M., Hovdebo, W., Cho, D., Jones, M., Maxwell, S., 2010, Surface seismic to microseismic: An integrated case study from exploration to completion in the Montney shale of NE British Columbia, Canada: 80th Annual International Meeting, SEG, Expanded Abstracts, 2095-2099.

Rüger, A., 1998, Variation of P-wave reflectivity with offset and azimuth in anisotropic media: Geophysics, vol. 63, no. 3, P. 935-947.

Schoenberg, M., and C. Sayers, 1995, Seismic anisotropy of fractured rock: Geophysics, 60, 204–211.

Sinha, B. K., Sayers, C., Endo, T., 2003, Determination of anisotropic moduli of Earth formations: US patent 2003/0167835 A1.

Thomsen, L., 1993, Weak anisotropic reflections, in Castagna, J. P., and Backus, M. M., Eds., Offset-dependent reflectivity—Theory and practice of AVO analysis: SEG, 103–111.

Vavryčuk, V., Pšenčík, I., 1998, PP-wave reflection coefficients in weakly anisotropic elastic media: Geophysics, vol. 63, no. 6, P. 2129-2141.